

This is a repository copy of *The impact of size and shape in the performance of hydrotropes : A case-study of alkanediols*.

White Rose Research Online URL for this paper:

<https://eprints.whiterose.ac.uk/184519/>

Version: Accepted Version

---

**Article:**

Abranches, Dinis O, Soares, Bruna P, Ferreira, Ana M et al. (3 more authors) (2022) The impact of size and shape in the performance of hydrotropes : A case-study of alkanediols. *Physical Chemistry Chemical Physics*. pp. 7624-7634. ISSN 1463-9084

<https://doi.org/10.1039/D2CP00496H>

---

**Reuse**

Items deposited in White Rose Research Online are protected by copyright, with all rights reserved unless indicated otherwise. They may be downloaded and/or printed for private study, or other acts as permitted by national copyright laws. The publisher or other rights holders may allow further reproduction and re-use of the full text version. This is indicated by the licence information on the White Rose Research Online record for the item.

**Takedown**

If you consider content in White Rose Research Online to be in breach of UK law, please notify us by emailing [eprints@whiterose.ac.uk](mailto:eprints@whiterose.ac.uk) including the URL of the record and the reason for the withdrawal request.

# The Impact of Size and Shape in the Performance of Hydrotropes: A Case-Study of Alkanediols

Dinis O. Abranches,<sup>1†</sup> Bruna P. Soares,<sup>1†</sup> Ana M. Ferreira,<sup>1</sup> Seishi Shimizu,<sup>2</sup> Simão P. Pinho,<sup>3</sup> and  
João A. P. Coutinho\*<sup>1</sup>

<sup>1</sup>CICECO - Aveiro Institute of Materials, Department of Chemistry, University of Aveiro, Aveiro, Portugal.

<sup>2</sup>York Structural Biology Laboratory, Department of Chemistry, University of York, Heslington, York YO10 5DD, UK.

<sup>3</sup>CIMO, Polytechnic Institute of Bragança, Bragança, Portugal.

\*Corresponding Author: João A. P. Coutinho (jcoutinho@ua.pt)

† Equally contributing authors

## Abstract

Inspired by the recently proposed cooperative mechanism of hydrotropy, where water molecules mediate the aggregation of hydrotrope around the solute, this work studies the impact of apolar volume and polar group position on the performance of hydrotropes. To do so, the ability of two different families of alkanediols (1,2-alkanediols and 1,n-alkanediols) to increase the aqueous solubility of syringic acid is initially investigated. Interestingly, it is observed that in the dilute region (low hydrotrope concentration), the relative position of the hydroxyl groups of the alkanediols does not impact their performance. Instead, their ability to increase the solubility of syringic acid correlates remarkably well with the size of their alkyl chains. However, this is not the case for larger hydrotrope concentrations, where 1,2-alkanediols are found to perform, in general, better than 1,n-alkanediols. These seemingly contradictory findings are reconciled using theoretical and experimental techniques, namely the cooperative model of hydrotropy and chemical environment probes (Kamlet-Taft and pyrene polarity scales). It is found that the number of hydrotropes aggregated around a solute molecule does not increase linearly with the apolar volume of the former, reaching a maximum instead. This maximum is discussed in terms of competing solute-hydrotrope and hydrotrope-hydrotrope interactions. The results suggest that hydrotrope self-aggregation is more prevalent in 1,n-alkanediols, which negatively impacts their performance as hydrotropes. The results reported in this work support the cooperative model of hydrotropy and, from an application perspective, show that hydrotropes should be designed taking into consideration not only their apolar volume but also their ability to stabilize their self-aggregation in water, which negatively impacts their performance as solubility enhancers.

## Introduction

Following the principles of Green Chemistry,<sup>1</sup> water is undoubtedly the most sustainable solvent: it is readily available, non-flammable, non-toxic, cheap, and environmentally benign. Unfortunately, many compounds that possess relevant properties and bioactivities display poor aqueous solubility. Rather than using different solvents to process these compounds, hydrotropes can be used to overcome this limitation. Hydrotropes are amphiphilic organic substances that significantly increase the aqueous solubility of hydrophobic compounds.<sup>2-4</sup> Since the concept was first proposed,<sup>5</sup> a variety of substances have been studied as hydrotropes, namely organic sulfonate salts,<sup>6</sup> glycerol ethers and esters,<sup>7-9</sup> ionic liquids,<sup>10-12</sup> and even simple organic molecules such as ethanol and urea.<sup>13</sup>

In contrast with surfactants, hydrotropes do not form well-structured aggregates such as micelles, and their mechanism of action is still not fully understood. After much speculation in the literature, the statistical thermodynamics-based cooperative model of hydrotropy<sup>14</sup> was recently proposed and experimentally confirmed by proton nuclear magnetic resonance (<sup>1</sup>H-NMR).<sup>15</sup> Within the framework of this model, a hydrotrope increases the solubility of a hydrophobic substance by aggregating around it in solution through its apolar moieties (hydrophobic effect). This aggregation is water-mediated, in the sense that aggregation between the apolar moieties of both hydrotrope and solute maximizes hydrogen bond-type interactions between water molecules or between water and hydrotrope. As such, the hydrotropic effect can be heightened by carefully selecting hydrotropes with large apolar volumes that still retain aqueous solubility.

Given the dependence of hydrotropy on the apolar volumes of solute and hydrotrope, families of compounds that possess easily tuned apolarity are a powerful tool to understand the overall mechanism of this phenomenon and rationally design better green hydrotropes for specific applications. For instance, while investigating the ability of glycerol and glycerol-derivatives to enhance the aqueous solubility of syringic acid, increasing the size of the alkyl side chain of monoglycerol ethers provided key insight into the mechanism of hydrotropy,<sup>7,15</sup> revealing that the magnitude of the solubility enhancement of a given solute correlates well with the apolarity of the hydrotrope and reaches a maximum when the apolar surface area of the hydrotrope and solute match. However, whether this is a general trend for all hydrotrope-solute pairs or a phenomenon specific to glycerol ethers is still unclear.

Alkanediols are a family of compounds that possess similar structures and amphiphilicity to monoglycerol ethers yet are structurally simpler and offer an additional array of tuning opportunities, namely the size of their alkyl chain and the position of their hydroxyl groups. As such, and considering the recent success of glycerol ethers highlighted in the previous paragraph, alkanediols offer the most valuable opportunity to systematically study the combined effects of hydrophobic and hydrophilic interactions in hydrotropy. Furthermore, alkanediols present a certain degree of sustainability, with many being FDA-approved and widely used in the cosmetic, food, and pharmaceutical industries.<sup>16</sup>

They have also been used to prepare sustainable deep eutectic solvents that extract and recover bioactive compounds from natural sources with high overall efficiency.<sup>17</sup>

To assess the impact of the alkyl chain length (size) and relative position of polar groups (shape) of hydrotropes on the solubility enhancement of hydrophobic solutes, the ability of two sets of alkanediols (1,2-alkanediols and 1,n-alkanediols with alkyl chain sizes ranging from one to seven carbons) to increase the aqueous solubility of syringic acid is investigated in this work. Alkanediols were chosen as model hydrotropes due to their tuning potential and sustainable character described above. Syringic acid was selected as the model solute due to its hydrophobicity, therapeutic activity, and presence in bio-relevant natural sources where sustainable extraction processes are desirable.<sup>18</sup> In fact, syringic acid is an antioxidant and an anti-inflammatory, while also functioning as a therapeutic agent for a wide range of diseases, such as cancer and diabetes. It can be found in several plants, ranging from grapes and olives to natural products such as honey, and functions as a surrogate of lignin (of which it is a monomer) in solubility studies. The solubility results obtained are modeled and interpreted in light of the Setschenow correlation and cooperative model of hydrotrophy. The Kamlet-Taft<sup>19</sup> and  $P_y$ <sup>20</sup> polarity scales are measured and used to rationalize the results obtained. To better understand the impact of the hydrophobicity of the solute in its interactions with the hydrotrope, two additional solutes with large apolar volumes are also studied (Reichardt's dye and pyrene).

## Experimental Section

### Chemicals

The chemical substances used in this work are listed in Table 1, along with their CAS number, source, and mass purity. The generic chemical structures of 1,2-alkanediols and 1,n-alkanediols, and the chemical structure of syringic acid are depicted in Figure 1 (see Figure S1 for a full list of chemical structures). The water used in all solubility essays was double distilled, passed across a reverse osmosis system, and treated with a Milli-Q plus 185 water purification apparatus.

**Table 1.** List of substances experimentally used in this work, along with their CAS number, supplier, and mass purity.

Substance	CAS number	Source	Purity (wt %)
1,2-Ethanediol	107-21-1	Fisher	>99.0
1,2-Propanediol	57-55-6	Sigma-Aldrich	99.5
1,3-Propanediol	504-63-2	Sigma-Aldrich	>98.0
1,2-Butanediol	584-03-2	Sigma-Aldrich	>98.0
1,4-Butanediol	110-63-4	Alfa Aesar	>99.0
1,2-Pentanediol	5343-92-0	TCI	97.0
1,5-Pentanediol	111-29-5	Alfa Aesar	97.0
1,2-Hexanediol	6920-22-5	Alfa Aesar	97.0
1,6-Hexanediol	629-11-8	Acros Organics	97.0
1,7-Heptanediol	629-30-1	TCI	>98.0
Syringic acid	530-57-4	Acros Organics	>98.0
Reichardt's dye	10081-39-7	Sigma-Aldrich	90.0
Pyrene	129-00-0	Sigma-Aldrich	>99.0
N,N-diethyl-4-nitroaniline	2216-15-1	Fluorochem	>99.0

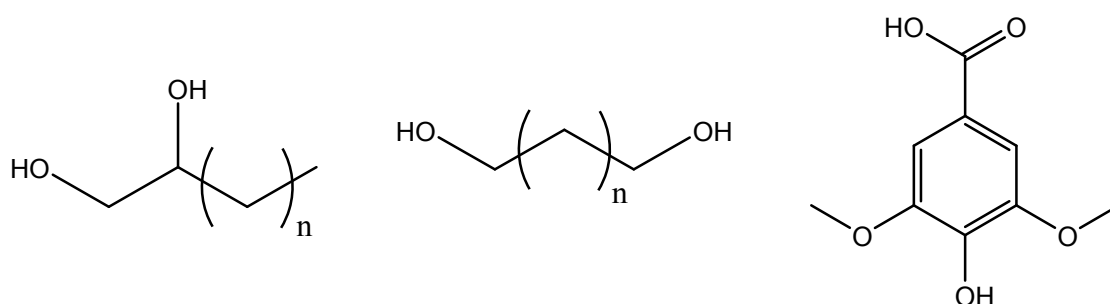


**Figure 1.** Generic chemical structures of 1,2-alkanediols (left,  $n=0$  to 3) and 1,n-alkanediols (middle,  $n=0$  to 5), and the chemical structure of syringic acid (right).

### **Solubility Curves**

The solubility of syringic acid in each water/hydrotrope solution was measured using the analytical isothermal shake-flask methodology.<sup>21</sup> Syringic acid was added in slight excess to each aqueous solution of hydrotrope or pure hydrotrope. The samples were equilibrated in an air oven at  $(303.2 \pm 0.5)$  K under constant stirring (1050 rpm) for 72 h, using an Eppendorf Thermomixer Comfort equipment. After 72 h, all samples were centrifuged at  $(303.2 \pm 0.5)$  K and 4500 rpm for 20 minutes in order to separate the excess undissolved solute from the liquid phase. Then, liquid-phase samples were carefully collected, filtered using syringe filters, and diluted in ultra-pure water. The amount of syringic acid was quantified by UV-spectroscopy using a SHIMADZU UV-1700 Pharma-Spec spectrometer at 267 nm. The solubility of syringic acid in pure water was found to be  $(1.462 \pm 0.004)$  g/L, in line with previous results reported in the literature.<sup>11,22</sup>

The procedure described above was also used to measure the solubility of Reichardt's dye and pyrene in aqueous solutions of 1,2-pentanediol or 1,5-pentanediol. Due to the high hydrophobicity of the solutes, the collected and filtered samples were diluted in water/ethanol 50% (v/v) and then quantified by UV-spectroscopy at 304 nm and 335 nm, respectively. The solubility of Reichardt's dye in pure water was found to be  $(30.8 \pm 0.5)$  mg/L, while the solubility of pyrene in pure water ( $0.17$  mg/L) was taken from the literature.<sup>23</sup>

### **Cooperative Model of Hydrotropy**

The solubility data for syringic acid obtained in this work was fitted using the cooperative model of hydrotropy, a statistical thermodynamics-based model developed by Shimizu and Matubayasi.<sup>14</sup> This model is based on solute-hydrotrope aggregation in solution and was developed for sigmoidal-shaped solubility curves. It can be summarized as:

$$\ln \left[ \frac{1 - \frac{S}{S_0}}{\frac{S}{S_0} - \left(\frac{S}{S_0}\right)_{max}} \right] = m \ln(x_H) + b \quad (1)$$

where  $S$  and  $S_0$  are the molar solubilities (mol/L) of the solute in the aqueous hydrotrope solution, or pure water, respectively,  $(S/S_0)_{max}$  is the maximum attainable relative solubility caused by a given hydrotrope,  $x_H$  is the mole fraction of the hydrotrope in the ternary water/hydrotrope/solute solution, and  $m$  and  $b$  are fitted parameters of the model.

Equation 1 is often fitted against solubility data by leaving  $(S/S_0)_{max}$  as an adjustable parameter as well.<sup>22</sup> This is done because most experimental solubility curves are not perfectly sigmoidal, with some presenting an absolute maximum, casting doubt on the ability to determine a value for  $(S/S_0)_{max}$  correctly. To avoid this problem and given that some of the solubility curves obtained in this work are not sigmoidal, this procedure is adopted here.

### Solvent Polarity Scales

The Kamlet-Taft solvatochromic parameter  $\pi^*$  (solvent dipolarity/polarizability)<sup>19</sup> and the *Py* scale parameter  $I_1/I_3$  (ratio between the first and third bands of the fluorescence spectrum of pyrene)<sup>20</sup> were experimentally measured in this work for aqueous solutions of 1,2-pentanediol or 1,5-pentanediol.

The solvatochromic parameter  $\pi^*$  was measured using the dye N,N-diethyl-4-nitroaniline. After vigorous stirring for the complete dissolution of the dye, samples were scanned using a UV-Vis spectrophotometer (BioTeck Synergy HT microplate reader). The longest wavelength absorption band was used to determine the parameter using the following equation:

$$\pi^* = \frac{\nu_{alkanediol} - \nu_{ciclohexane}}{\nu_{DMSO} - \nu_{ciclohexane}} \quad (2)$$

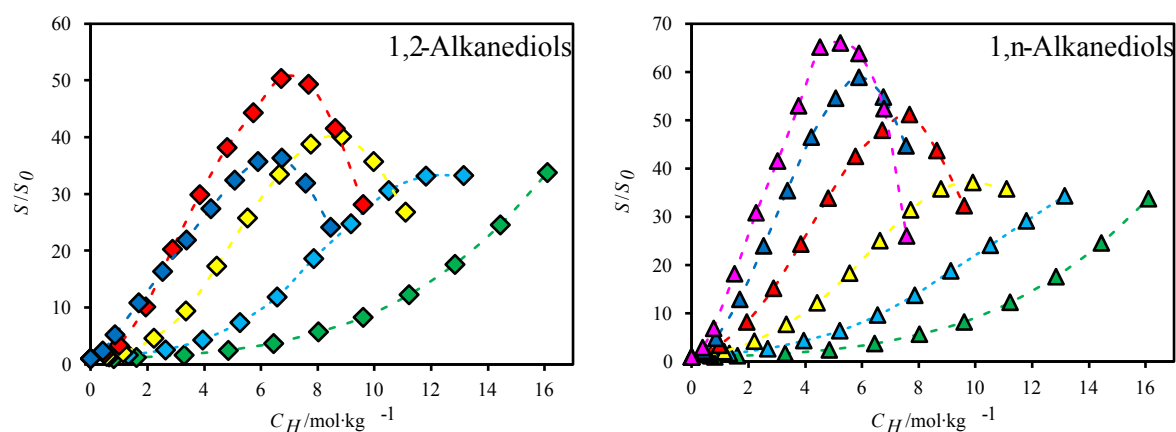
where  $\nu$  is the experimental wave number and the subscripts *alkanediol*, *ciclohexane*, and *DMSO* correspond to the solvent used.

To measure the polarity index ( $I_1/I_3$ ), fluorescence measurements using pyrene were carried out, as previously described in the literature.<sup>20,24–26</sup> The fluorescence emission spectra were obtained with aerated solutions at very low pyrene concentration ( $3 \cdot 10^{-7}$  mol/L), which ensured the absence of pyrene excimers. Adequate volumes of pyrene in ethanol solutions were transferred to empty Eppendorf vessels and the solvent was carefully evaporated. The aqueous solutions of alkanediols (1,2 and 1,5-pentanediol) were then added. In order to ensure equilibrium, the spectra were measured after 48 h of constant stirring (2000 rpm) using an Eppendorf Thermomixer Comfort equipment. The pyrene spectra were quantified using a JASCO FP-8300 spectrofluorometer at an excitation wavelength of 318 nm. The spectra were used to determine the ratio of the intensities of the first and third vibronic peaks of monomeric pyrene (polarity index,  $I_1/I_3$ ).

## Results and Discussion

### Solubility Curves of Syringic Acid

The solubility curves of syringic acid in aqueous solutions of 1,2-alkanediols and 1,n-alkanediols, measured in this work, are depicted in Figure 2. Detailed experimental results are reported in Supporting Information (Tables S1 and S2). The solubility of syringic acid was measured in the entire experimentally available concentration range of the hydrotrope, from pure water to pure hydrotrope or its aqueous solubility limit.



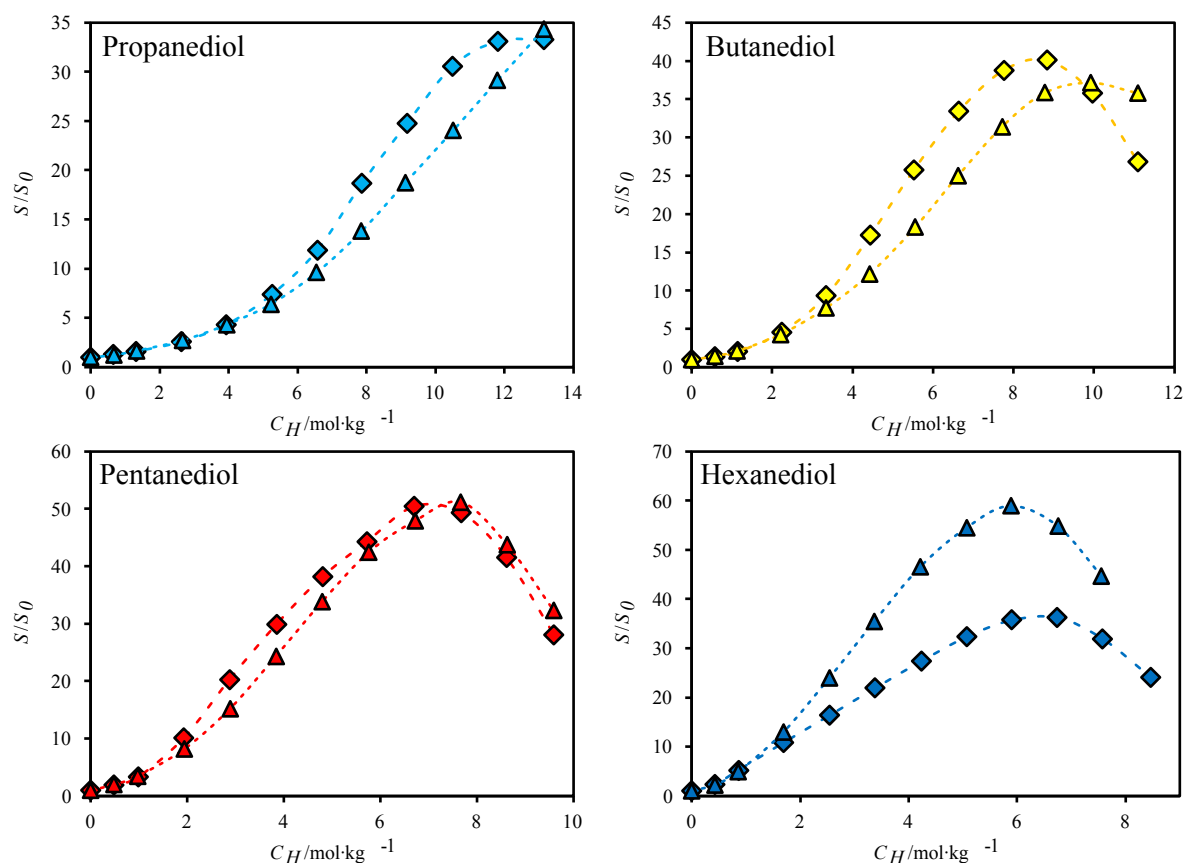
**Figure 2.** Solubility enhancement of syringic acid in aqueous solutions of 1,2-ethanediol  $\blacklozenge$  or  $\blacktriangle$ , 1,2-propanediol  $\blacklozenge$ , 1,2-butanediol  $\blacklozenge$ , 1,2-pentanediol  $\blacklozenge$ , 1,2-hexanediol  $\blacklozenge$ , 1,3-propanediol  $\blacktriangle$ , 1,4-butanediol  $\blacktriangle$ , 1,5-pentanediol  $\blacktriangle$ , 1,6-hexanediol  $\blacktriangle$ , and 1,7-heptanediol  $\blacktriangle$  as a function of hydrotrope concentration, at 303.2 K.  $S/S_0$  is the relative solubility of syringic acid and  $C_H$  is the concentration of hydrotrope per kg of solution (solute-free basis). Dashed lines are visual guides.

Figure 2 reveals that the aqueous solubility of syringic acid can be increased up to 60-fold using alkanediols as hydrotropes. This value is similar to that obtained with other nonionic hydrotropes previously studied, such as glycerol ethers (up to 77-fold for 1,3-dimethoxy-2-propanol)<sup>7</sup> and Cyrene (up to 45-fold).<sup>22</sup> Furthermore, the performance of alkanediols is superior to ionic hydrotropes with densely charged counterions, such as the prototypical 1-butyl-3-methylimidazolium chloride (which enhances the aqueous solubility of syringic acid up to 40-fold), but inferior to ionic hydrotropes containing amphiphilic counter ions, such as 1-butyl-3-methylimidazolium p-toluenesulfonate that reached a 170-fold solubility improvement.<sup>11</sup>

Except for 1,2-hexanediol, the results depicted in Figure 2 reveal that the solubility enhancement of syringic acid generically increases with the size of the alkyl chain of the hydrotrope, up to a hydrotrope concentration of 6 mol/kg. This trend is in line with the recently proposed molecular mechanism of hydrotropy, where the apolar volume of the hydrotrope is one of the main driving forces of hydrotropy.<sup>14,15</sup> However, between hydrotrope concentrations of 6 and 9 mol/kg, the solubility of syringic acid reaches a maximum for hydrotropes with larger alkyl chains, decreasing afterward. This is most likely due to a change in the solvation regime, as will be discussed in the following sections.



Although both families of hydrotropes display the same apolar volume trend, as discussed in the previous paragraph, the position of the hydroxyl group appears to impact their performance. To better showcase this, the data reported in Figure 2 are replotted in Figure 3 to highlight the differences between the performances of 1,2-alkanediols and 1,n-alkanediols.



**Figure 3.** Solubility enhancement of syringic acid in aqueous solutions of propanediol (1,2-propanediol  $\blacklozenge$  and 1,3-propanediol  $\blacktriangle$ ), butanediol (1,2-butanediol  $\blacklozenge$  and 1,4-butanediol  $\blacktriangle$ ), pentanediol (1,2-pentanediol  $\blacklozenge$  and 1,5-pentanediol  $\blacktriangle$ ), and hexanediol (1,2-hexanediol  $\blacklozenge$  and 1,6-hexanediol  $\blacktriangle$ ), as a function of hydrotrope concentration, at 303.2 K.  $S/S_0$  is the relative solubility of the solute and  $C_H$  is the concentration of hydrotrope per kg of solution (solute-free basis). Dashed lines are visual guides.

The results depicted in Figure 3 reveal a curious trend. For shorter alkyl chains, 1,2-alkanediols outperform 1,n-alkanediols, with both 1,2-propanediol and 1,2-butanediol displaying higher solubility enhancements than 1,3-propanediol and 1,4-butanediol, respectively. However, the trend is inverted for larger alkyl chains. While there is no noticeable difference between the performances of 1,2-pentanediol and 1,5-pentanediol, 1,6-hexanediol can achieve a greater syringic acid solubility enhancement (up to 60-fold) than 1,2-hexanediol (up to 40-fold). This clearly shows that the relative position of polar groups in hydrotropes impacts their ability to enhance the aqueous solubility of hydrophobic solutes, although the reason for this phenomenon is not yet clear.

### The Dilute Region

The interpretation of the effect that the relative position of hydroxyl groups in alkanediols has on hydrotrophy is made difficult by the diversity of possible interactions that can be established between water, hydrotrope, and solute, each playing favorable or unfavorable roles towards the solubility enhancement of the solute. While this is certainly true for larger concentrations of hydrotrope, in the dilute region (i.e., low hydrotrope concentration) the contribution to solubilization from hydrotrope-hydrotrope and solute-solute interactions has been shown to be greatly decreased.<sup>4</sup> Thus, studying the dilute region should provide important clues to understand solute-hydrotrope interactions.

The Setschenow constant ( $K_S$ ) quantifies the solubility enhancement of a substance due to the addition of a third component (e.g. hydrotrope, cosolvent, salt, etc.) in the dilute region.<sup>27,28</sup> In this work, it is defined as:

$$\ln(S/S_0) = K_S \cdot C_H \quad (3)$$

where  $S$  and  $S_0$  are the molar solubilities (mol/L) of the solute in the aqueous hydrotrope solution and pure water, respectively, and  $C_H$  is the concentration (mol/kg<sub>solution</sub>) of the hydrotrope in a solute-free basis.

Equation 3 was initially proposed by Setschenow<sup>27</sup> to quantify salting-out and salting-in effects but has since proved useful in the field of hydrotrophy.<sup>4,7,22</sup> Note that this equation is, in essence, a linear correlation between  $\ln(S/S_0)$  and  $C_H$ , and is only valid when these variables possess a linear relationship (i.e., the dilute region). In this work, this was found to be true up to about 20 wt%, depending on the hydrotrope. As such, each solubility curve reported in the previous section was fitted using Equation 3 in the dilute region, and the results obtained are depicted in Figure 4.

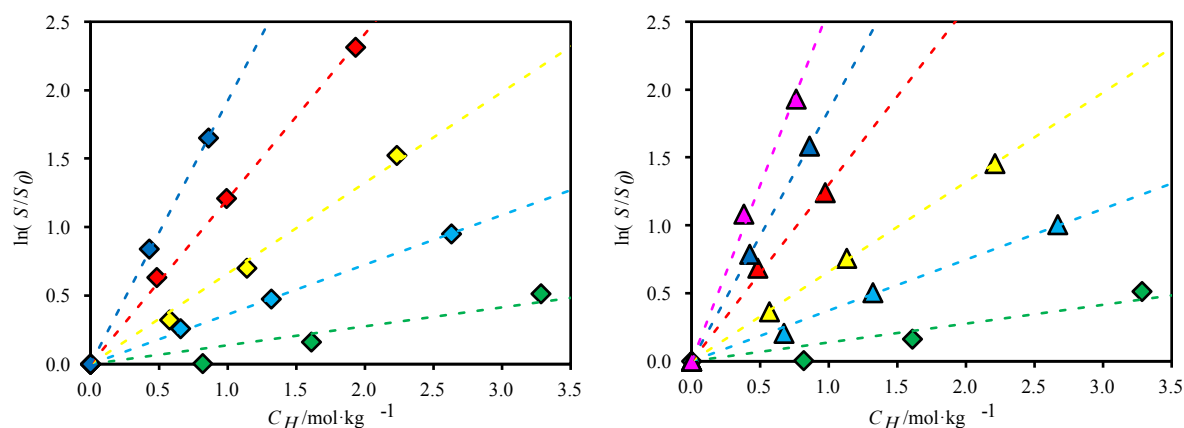


**Figure 4.** Natural logarithm of the relative solubility enhancement of syringic acid, at 303.2 K, as a function of the concentration of hydrotrope for 1,2-alkanediols (left) and 1,n-alkanediols (right), in particular 1,2-ethanediol  $\blacklozenge$ , 1,2-propanediol  $\blacklozenge$ , 1,2-butanediol  $\blacklozenge$ , 1,2-pentanediol  $\blacklozenge$ , 1,2-hexanediol  $\blacklozenge$ , 1,3-propanediol  $\blacktriangle$ , 1,4-butanediol  $\blacktriangle$ , 1,5-pentanediol  $\blacktriangle$ , 1,6-hexanediol  $\blacktriangle$  and 1,7-heptanediol  $\blacktriangle$ . Dashed lines represent the best linear fitting for each data set obtained using the least square method and setting the intercept to zero.

Figure 4 reinforces the conclusions presented in the previous section: the ability of each hydrotrope to increase the solubility of syringic acid correlates positively with the size of their alkyl chain. In other words, the larger the apolar volume of the hydrotrope, the larger the solubility enhancement in the dilute region. Thus, while 1,2-pentanediol is, surprisingly, better than 1,2-hexanediol at higher concentrations, both hydrotropes follow the general apolar trend in the dilute region.

Besides the impact of the apolar volume, the results discussed in the previous section suggest that the relative position of the hydroxyl groups has an impact on the performance of alkanediols as hydrotropes. To evaluate whether this phenomenon is present in the dilute region, the Setschenow constant (slope of each curve depicted in Figure 4) is now correlated against a metric that quantifies the apolar volume of the hydrotrope. Given the structural similarity of the alkanediols studied in this work, their molar mass (or their number of carbon atoms) is a good surrogate for their apolar volume. In this sense, Figure 5 depicts the Setschenow constants as a function of the molar mass of the hydrotrope, for the two hydrotrope series. The numerical values are reported in Table S5 of the Supporting Information.

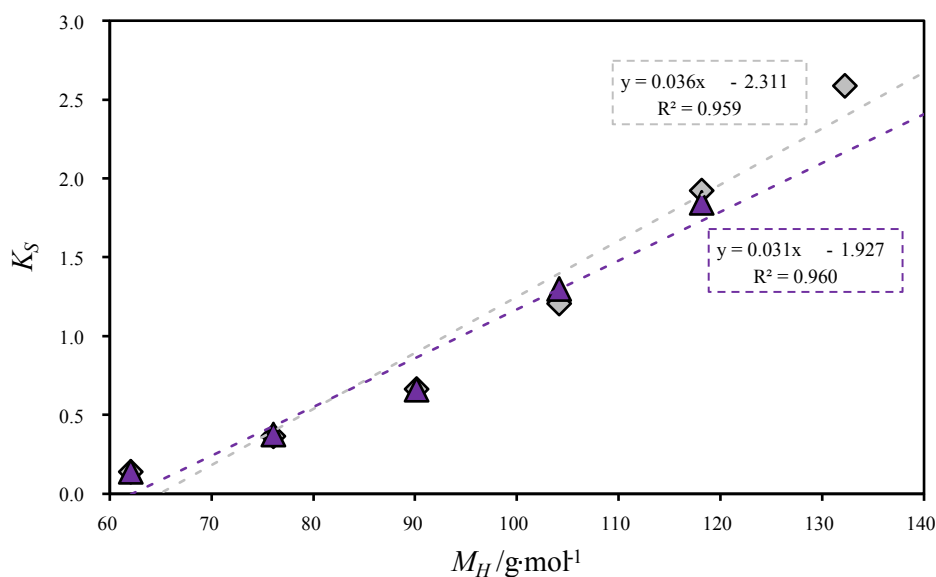


**Figure 5.** Setschenow constant ( $K_S$ ) as a function of the hydrotrope molar mass ( $M_H$ ) for 1,2-alkanediols ( $\diamond$ ) and 1,n-alkanediols ( $\blacktriangle$ ). Dashed lines represent the best linear fitting obtained using the least square method.

As expected from the results reported in Figures 2 and 4, Figure 5 reinforces the positive correlation between the performance of alkanediols as hydrotropes (here quantified by the Setschenow constant) and their apolar volume (here quantified by their molar mass). More interestingly, Figure 5 reveals that in the dilute region, from where the Setschenow constants were estimated, there are no significant differences in the hydrotropic effect of the two series of alkanediols as the lines practically overlap. In fact, the standard deviations associated with the slopes shown in Figure 5 are 0.0043 and 0.0034 for the 1,2 and 1,n-alkanediol sets, respectively. These very small standard deviations, when compared to the difference between the two slopes, show them to be statistically the same at a 5% significance level (significance = 0.512 > 0.05). This is in direct conflict with the observations of the previous section,

where the relative position of the hydroxyl groups was found to have an impact on hydrotropy, with 1,2-alkanediols performing better than 1,n-alkanediols for shorter alkyl chains but worse for longer alkyl chains.

The fact that the hydroxyl position appears to impact hydrotropy only for larger concentrations of hydrotrope but not in the dilute region suggests that its effect may stem from interactions that are heightened by the presence of the hydrotrope. In other words, this suggests that hydrotrope-hydrotrope interactions, whose presence is expected to be more significant at higher hydrotrope concentrations, are the reason behind the performance differences between the dilute and non-dilute regions.

It is worth noting that the Setschenow constant, as defined in Equation 3, is proportional to the difference between the Kirkwood-Buff (KB) integrals of solute and hydrotrope ( $G_{S,H}$ ) and of solute and water ( $G_{S,W}$ ):<sup>29</sup>

$$K_S \propto G_{S,H} - G_{S,W} \quad (4)$$

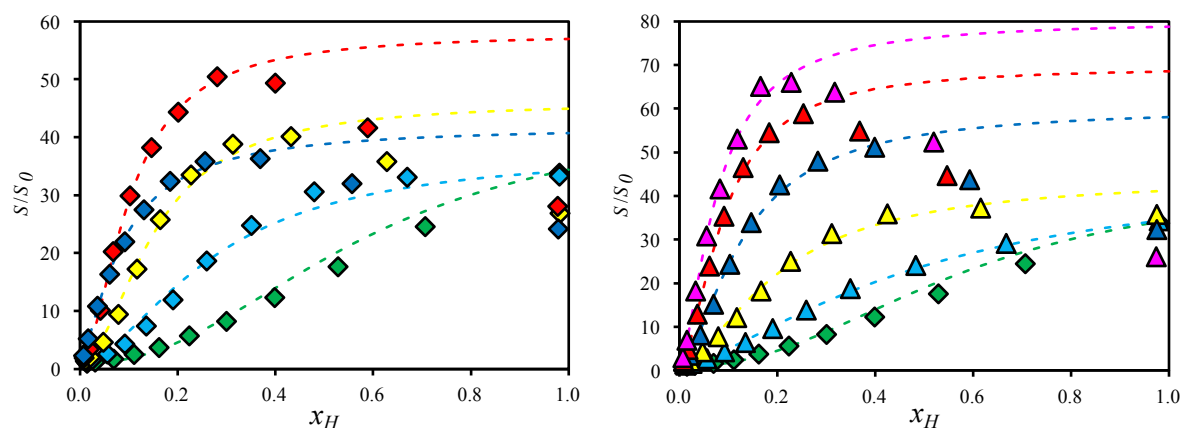
The KB integrals quantify the excess of a component in the local vicinity of another component. As such,  $G_{S,H}$  quantifies the excess of hydrotrope around the solute and  $G_{S,W}$  quantifies the excess of water around the solute. Put differently, the difference between these KB integrals, which is proportional to  $K_S$ , measures the preference of the solute to be surrounded by hydrotrope rather than water. The results depicted in Figure 4 show that the Setschenow constant increases with the apolar volume of the hydrotrope. This, once more, supports the current understanding of the mechanism of hydrotropy:<sup>14,15</sup> as the apolar volume of the hydrotrope increases, so does the driving force for aggregation around the solute. Thus,  $G_{S,H}$  increases, leading to larger hydrotrope-solute clusters and better solubility enhancements of the solute.

### **Cooperative Model of Hydrotropy**

The results discussed in the previous two sections reveal interesting and somewhat contradictory phenomena:

- (i) In the dilute region, the performance of alkanediols correlates with their apolar volume, and the relative position of their hydroxyl groups has no impact;
- (ii) In the non-dilute region, the performance of alkanediols somewhat correlates with their apolar volume (except for 1,2-hexanediol), yet the relative position of their hydroxyl groups has an impact on their performance, which depends on the size of their alkyl chains (the performance of 1,2-hexanediol is inferior to the performances of 1,2-butanediol and 1,2-pentanediol, and the performance of 1,6-hexanediol is largely superior to that of 1,2-hexanediol).

To shed light on the origins of these discrepancies, a more holistic approach in the form of the cooperative model of hydrotrophy is used in this section. This model, which has strong statistical thermodynamics foundations and has been experimentally validated,<sup>14,15</sup> is used in this section to fit all the syringic acid solubility curves measured in this work. Note that hydrotrope concentrations (solute-free basis) were converted to ternary mole fractions and that the fitting was carried out using the solubility data up to the solubility maxima. These results are depicted in Figure 6, and the fittings are reported in Figures S2-S3 and Table S6 of the Supporting Information.



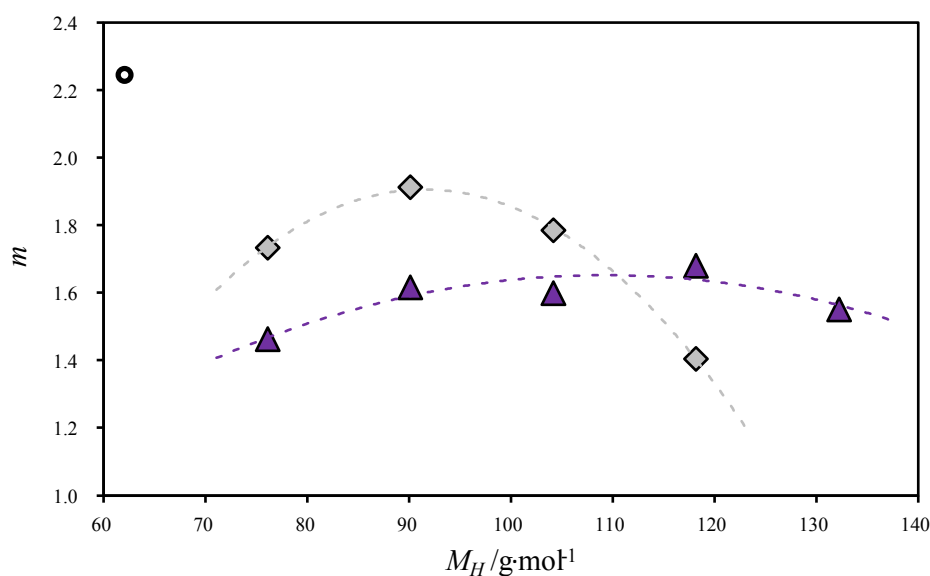
**Figure 6.** Relative solubility enhancement ( $S/S_0$ ) of syringic acid, at 303.2 K, as a function of ternary hydrotrope mole fraction, for 1,2-alkanediols (left) and 1, $n$ -alkanediols (right), in particular 1,2-ethanediol  $\blacklozenge$ , 1,2-propanediol  $\blacklozenge$ , 1,2-butanediol  $\blacklozenge$ , 1,2-pentanediol  $\blacklozenge$ , 1,2-hexanediol  $\blacklozenge$ , 1,3-propanediol  $\blacktriangle$ , 1,4-butanediol  $\blacktriangle$ , 1,5-pentanediol  $\blacktriangle$ , 1,6-hexanediol  $\blacktriangle$  and 1,7-heptanediol  $\blacktriangle$ . Dashed lines represent the fitted curves obtained using the cooperative model of hydrotrophy.

Figure 6 shows that the cooperative model of hydrotrophy can accurately fit the solubility curves of all solute-hydrotrope pairs, until the solubility maximum of each curve is reached. It should be noted that, within the framework (and limitation) of the model, hydrotropic solubility curves cannot pass through local maxima. Thus, and according to the current understanding of the mechanism of hydrotrophy, the maxima displayed by some of the solubility curves reported in this work is related to a change in the solvation environment of the solute. At high concentrations of hydrotrope, water is no longer the major solvent of the system, and water-mediated hydrotrope-solute interactions lose importance, with the system transitioning from a hydrotrophy to a co-solvency regime.<sup>30</sup>

The parameter  $m$  of the cooperative model of hydrotrophy (see Equation 1) is related to the average number of hydrotropes that aggregate around a given molecule of solute. For syringic acid and glycerol ethers, this parameter was shown to be non-monotonous with respect to the apolarity of the hydrotrope, reaching a maximum when the apolarities of the solute and hydrotrope match.<sup>15</sup> This was interpreted in light of competing interactions, as follows: From the perspective of water, there is no difference between the apolar moieties of the hydrotrope and the apolar moieties of the solute; as such, when the apolar volume of the hydrotrope is larger than the apolar volume of the solute, the driving force (hydrophobic effect) for hydrotrope-hydrotrope aggregation is larger than the driving force for solute-hydrotrope

aggregation. This decreases the average number of available hydrotropes to aggregate around the solute (parameter  $m$ ). However, this does not necessarily translate into a decrease in hydrotropic efficiency, as even though a more apolar hydrotrope may be statistically less aggregated around a solute, they can cover more of the apolar area of the solute given their larger apolar volume.

To check whether the phenomenon discussed in the previous paragraph is also present in the systems studied in this work, the  $m$  parameters here obtained (see Table S6 of Supporting Information) are now correlated against the apolarity of the alkanediols (in line with Figure 5, the apolarity is quantified by the molar mass of the hydrotrope). These results are depicted in Figure 7.



**Figure 7.** Parameter  $m$  of the cooperative model of hydrotropy as a function of the hydrotrope molar mass ( $M_H$ ) for 1,2-alkanediols (◇), 1,n-alkanediols (▲), and 1,2-ethanediol (●). The dashed lines represent quadratic fittings obtained using the method of least squares.

Figure 7 reveals several interesting phenomena. To start, parameter  $m$  of the cooperative model of hydrotropy clearly reaches a maximum as a function of the apolar volume of the hydrotrope for both families of alkanediols. This phenomenon has also been observed for monoglycerol ethers,<sup>15</sup> which suggests that this is a general trend of hydrotropy and not a peculiarity of alkanediols. However, the position and shape of the maxima are different for both series of alkanediols. The maximum for 1,2-alkanediols occurs at a smaller hydrotrope apolar volume when compared to the maximum of the 1,n-alkanediols. Surprisingly, 1,2-ethanediol clearly does not fit the quadratic trend observed in Figure 7, which suggests that its ability to enhance the solubility of syringic acid arises from a mechanism other than cooperative hydrotropy. The nature of this mechanism and how it relates to hydrotropy will be the object of future work.

The observation made in the previous sections that 1,2-butanediol and 1,2-pentanediol outperform 1,2-hexanediol in the non-dilute region, despite possessing smaller apolar volumes, can now be interpreted considering the results depicted in Figure 7. Because  $m$  reaches a maximum for 1,2-butanediol in the

1,2-alkanediol series, both 1,2-pentanediol and 1,2-hexanediol are statistically less aggregated around the solute than their less apolar counterparts. If the maximum of parameter  $m$  is rationalized in terms of competing interactions as discussed above (the driving force for hydrotrope-hydrotrope aggregation becomes larger than the driving force for solute-hydrotrope aggregation), it means that the driving force for hydrotrope-hydrotrope aggregation is greater in aqueous solutions of 1,2-pentanediol and 1,2-hexanediol. While for 1,2-pentanediol this is not enough to be noticeable in its performance as a hydrotrope for syringic acid, it is enough to greatly decrease the amount of 1,2-hexanediol aggregated around the solute, leading to lower hydrotropic performance. This also explains why this effect is not seen in the dilute region (Figures 3 and 4): Since 1,2-hexanediol is outperformed due to its tendency to self-aggregate, this effect is only noticeable when hydrotrope-hydrotrope interactions become more likely (i.e., non-dilute region), and does not impact the dilute region performance.

Having interpreted the discrepancy between the dilute and non-dilute regions regarding the relationship between apolar volume and hydrotrope performance, now the impact of the relative position of the hydroxyl groups is explored. As shown in Figure 7,  $m$  is generally smaller for 1, $n$ -alkanediols than 1,2-alkanediols. The position of the maximum of this parameter, which is connected to the apolarity of the solute as discussed above,<sup>15</sup> is also shifted, occurring at larger molar masses for the 1, $n$ -alkanediol family. Again considering that the extent of solute-hydrotrope aggregation (quantified by  $m$ ) is a balance between the driving forces for solute-hydrotrope and hydrotrope-hydrotrope aggregation, these observations suggest that, compared to 1,2-alkanediols, 1, $n$ -alkanediols are either more prone to bulk-phase self-aggregation or less prone to aggregate around the solute.

Due to the relative position of their hydroxyl groups, the most energetically favorable dimer of 1, $n$ -alkanediols is an antiparallel conformation, while 1,2-alkanediols are more prone to head-to-head dimerization.<sup>31</sup> From the standpoint of water, parallel aggregation of large alkyl chains is more favorable than head-to-head because it covers a larger apolar area (hydrophobic effect), maximizing the number of water-water contacts. This, together with the fact that the enthalpies of vaporization of 1, $n$ -alkanediols are superior to those of 1,2-alkanediols,<sup>32,33</sup> suggests that 1, $n$ -alkanediols are more prone to self-aggregation in water than 1,2-alkanediols. In turn, this suggests that the  $m$  discrepancy between both families of alkanediols is related to hydrotrope self-aggregation, not solute-hydrotrope interactions.

### **Polarity Probes and Local Environment**

The previous section reconciled the relationship between the apolar volume of the hydrotrope and the solubility enhancement of the solute in the dilute and non-dilute regions while providing a hypothesis to explain the different performances of 1,2-alkanediols and 1, $n$ -alkanediols. Now, two experimental polarity scales are explored to provide further insight on how alkanediols interact with the solute and to validate the conclusions drawn above: the Kamlet-Taft solvatochromic parameter  $\pi^*$  (solvent

dipolarity/polarizability)<sup>19</sup> and the *Py* scale parameter  $I_1/I_3$  (ratio between the first and third bands of the fluorescence spectrum of pyrene).<sup>20</sup>

The polarity scales  $\pi^*$  and  $I_1/I_3$  were experimentally measured in this work, as described in the experimental section, for aqueous solutions of 1,2-pentanediol and of 1,5-pentanediol, in the entire experimentally available concentration range of the hydrotrope, from pure water to pure hydrotrope. These results are depicted in Figure 8 and reported in Tables S7 and S8 of Supporting Information. These two hydrotropes were chosen because they represent a compromise between the position of the maxima of parameter  $m$  for both alkanediol families and show the lower performance deviation for syringic acid (Figure 3).

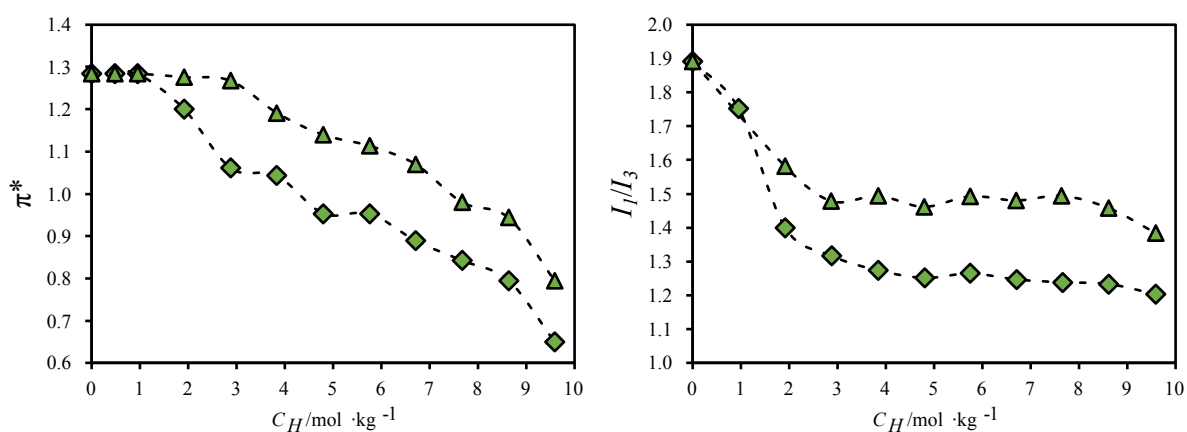


**Figure 8.** Kamlet-Taft solvatochromic parameter  $\pi^*$  (left) and the *Py* scale parameter  $I_1/I_3$  (right) for aqueous solutions of 1,2-pentanediol ( $\blacklozenge$ ) or 1,5-pentanediol ( $\blacktriangle$ ).  $C_H$  is the concentration of hydrotrope per kg of solution (solute-free basis). Dashed lines are visual guides.

Noting that both the Kamlet-Taft solvatochromic parameter  $\pi^*$  and the *Py* scale parameter  $I_1/I_3$  are proportional to the polarity of the solvent (larger values of  $\pi^*$  or  $I_1/I_3$  represent more polar or less apolar environments), Figure 8 unambiguously shows that aqueous solutions of 1,2-pentanediol are more apolar than aqueous solutions of 1,5-pentanediol, from the perspective of the molecular probe. In other words, the local environment of the probes used to measure these parameters maintains more apolar contacts in aqueous solutions of 1,2-pentanediol than in aqueous solutions of 1,5-pentanediol. This is in line with the hypothesis raised in the previous section to explain the impact of the relative position of hydroxyl groups in the performance of alkanediols as hydrotropes: because 1,5-pentanediol is more prone to self-aggregation in water, its apolar moieties are not as available to aggregate around hydrophobic molecules as those of 1,2-pentanediol. Note that the reduction of solubilization efficacy due to hydrotrope self-aggregation in water has been shown statistical thermodynamically using the Kirkwood-Buff integrals.<sup>4</sup> As such, from a designing standpoint, this shows that hydrotropes should be chosen not only taking into consideration their apolar volume but also their ability to stabilize their self-aggregation in water, which negatively impacts their performance as solubility enhancers.



Acree et al.<sup>34,35</sup> developed a method to estimate the local composition of pyrene in aqueous solutions using the *Py* scale parameter  $I_1/I_3$ , which has been tested for aqueous solutions of alcohols.<sup>26</sup> Briefly, the method assumes that  $I_1$  and  $I_3$  can be estimated by taking the composition average of these values in the pure solvents (water and hydrotrope). In other words:

$$\frac{I_1}{I_3} = \frac{x_H^L \cdot I_{1,H} + (1 - x_H^L) \cdot I_{1,W}}{x_H^L \cdot I_{3,H} + (1 - x_H^L) \cdot I_{3,W}} \quad (5)$$

where  $I_{1,H}$  and  $I_{3,H}$  are the intensities of the first and third bands of the fluorescence spectrum of pyrene dissolved in pure hydrotrope, respectively,  $I_{1,W}$  and  $I_{3,W}$  are the intensities of the first and third bands of the fluorescence spectrum of pyrene dissolved in pure water, respectively, and  $x_H^L$  is the local mole fraction of hydrotrope around pyrene in the ternary mixture (water/hydrotrope/pyrene). Using  $x_H^L$ , a metric that quantifies the excess of hydrotrope around the solute can be defined in terms of the difference between local and bulk hydrotrope compositions:

$$\delta_H = x_H^L - x_H \quad (6)$$

Equations 5 and 6 were used to calculate  $x_H^L$  and  $\delta_H$ , respectively, and the results are depicted in Figure 9 and reported in Tables S10 and S11 of Supporting Information.

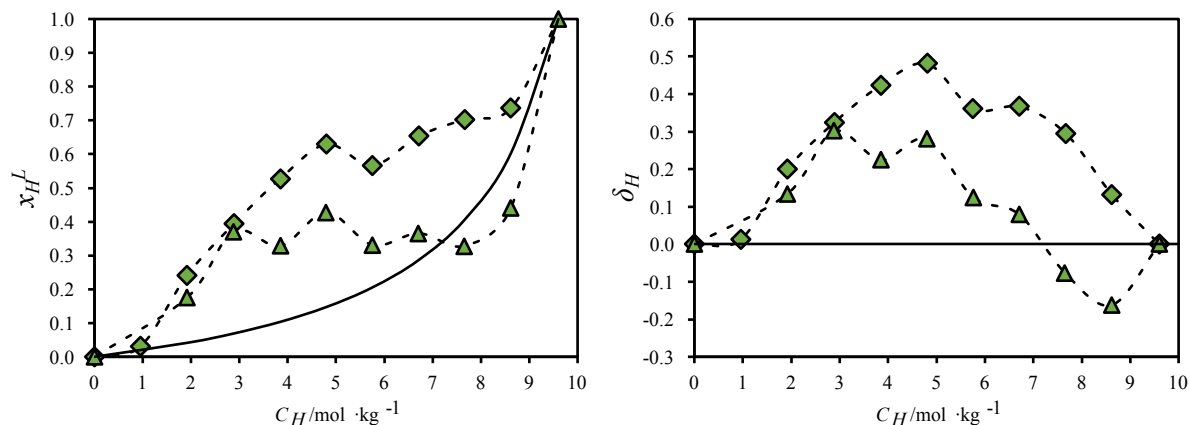


**Figure 9.** Local composition of hydrotrope around the pyrene probe (left) and difference between local and bulk compositions (right) for aqueous solutions of 1,2-pentanediol (◆) or 1,5-pentanediol (▲).  $C_H$  is the concentration of hydrotrope per kg of solution (solute-free basis). Dashed lines are visual guides and full lines represent thermodynamic ideality (local composition equal to bulk composition).

Even though the method used to estimate the local composition of hydrotrope around pyrene is quite sensitive to the uncertainty of the experimental  $I_1/I_3$  data, Figure 9 supports all the conclusions drawn in this work. In particular, the results depicted in Figure 9 show the preferential aggregation of hydrotrope around the apolar probe (pyrene): the local composition of hydrotrope is larger than its bulk composition in most of its concentration range. Furthermore, the local composition of 1,2-pentanediol is superior to that of 1,5-pentanediol, reinforcing that 1,n-alkanediols are more prone to self-aggregation

and, thus, less available to aggregate around hydrophobic solutes. Finally, the fact that the differences in local composition are mostly seen for larger hydrotrope concentrations reinforces the discrepancies observed between the non-dilute and dilute regions.

### **Highly hydrophobic solutes**

Although pyrene was used in the previous section in trace quantities to act as an apolarity probe, the results obtained clearly match the mechanism of hydrotropy (aggregation of hydrotrope around a hydrophobic molecule). As such, it is reasonable to speculate that alkanediols can act as hydrotropes and enhance the aqueous solubility of pyrene. In the final section of this work, the solubility of pyrene in aqueous solutions of 1,2- and 1,5-pentandiol is investigated. Seeing as pyrene is quite more hydrophobic than syringic acid, this presents an opportunity to assess the impact of the hydrophobicity of the solute on the performance of hydrotropes. Taking this into consideration, another solute, Reichardt's dye, was also tested. This solute was chosen due to the ease of its quantification using UV techniques despite its very low water solubility. The chemical structures of these two additional solutes are depicted in Figure 10.

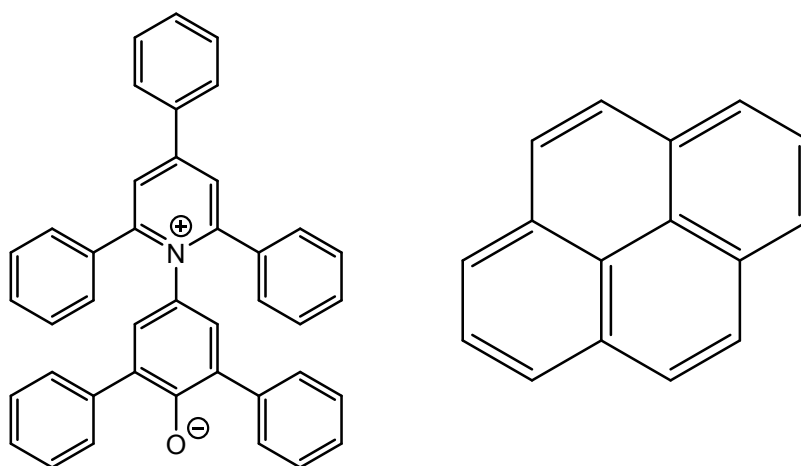


**Figure 10.** Chemical structure of Reichardt's dye (left) and pyrene (right).

To start this discussion, the solubility curves of Reichardt's dye and pyrene in aqueous solutions of 1,2-pentandiol and of 1,5-pentandiol, experimentally measured in this work, are depicted in Figure 11 and reported in Tables S3 and S4 of Supporting Information.

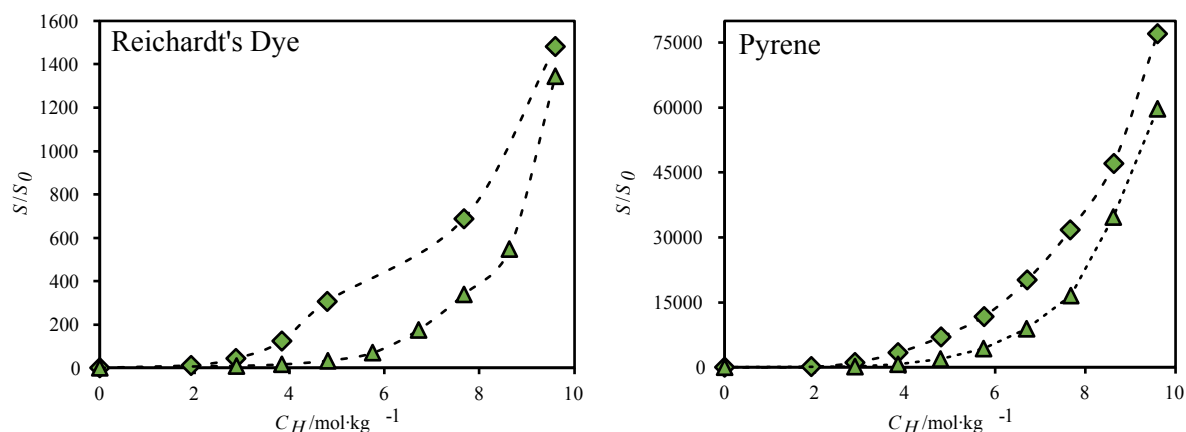


**Figure 11.** Solubility enhancement of Reichardt's Dye (left) and pyrene (right) in aqueous solutions of 1,2-pentandiol (◆) or 1,5-pentandiol (▲).  $C_H$  is the concentration of hydrotrope (solute-free basis). Dashed lines are visual guides.

As expected, Figure 11 shows that alkanediols are able to enhance the aqueous solubility of pyrene and Reichardt's dye. It is noteworthy that, for these more hydrophobic solutes, 1,2-pentandiol clearly performs better than 1,5-pentandiol, in contrast with the results obtained for syringic acid, where the differences are much less noticeable. This can be interpreted by considering the results depicted in Figure 7. As previously shown for glycerol ethers, parameter  $m$  of the cooperative model of hydrotrophy reaches a maximum when the apolarities of the solute and hydrotrope match.<sup>15</sup> Because for syringic acid the maximum of  $m$  is located at around the apolarities of 1,2- and 1,5-pentandiol, the maxima for these more hydrophobic solutes is expected to only be reached for larger hydrotropes. Thus, the differences in the performance of the pentanediols for these solutes should be similar to those observed in the smaller alkanediols for syringic acid.

## Conclusions

To assess the impact of the apolar volume and polar group position of hydrotropes in their ability to enhance the aqueous solubility of hydrophobic substances, two families of alkanediols were used in this work to increase the aqueous solubility of syringic acid. All alkanediols tested were able to act as hydrotropes, and the solubility of syringic acid could be enhanced up to 65-fold for the best-performing hydrotrope (1,7-heptanediol).

Using the empirical Setschenow model in the dilute hydrotrope concentration range, it was found that the ability of a hydrotrope to enhance the aqueous solubility of a hydrophobic substance correlates with its apolar volume, with larger alkanediols being able to achieve higher performances. The relative position of their hydroxyl groups was found to have no impact on their performance in the dilute region. This is in line with the cooperative mechanism of hydrotropy, which states that water, being highly polar and establishing strong hydrogen bonding with other water molecules, drives the apolar moieties of the hydrotrope to aggregate around hydrophobic solute molecules. On the other hand, in the non-dilute region, the performance of 1,2-hexanediol was found to be inferior to that of 1,2-butanediol and 1,2-pentanediol, and the performance of 1,6-hexanediol was largely superior to that of 1,2-hexanediol. This is intriguing, as the apolar volume of 1,2-hexanediol is larger than the apolar volumes of 1,2-butanediol and 1,2-pentanediol and equal to the apolar volume 1,6-hexanediol.

The contradictory observations made for 1,2-hexanediol were reconciled using the cooperative mechanism of hydrotropy that showed that the number of hydrotropes aggregated around the solute did not increase linearly with the apolar volume of the hydrotrope, reaching a maximum instead. This maximum was interpreted in light of competing solute-hydrotrope and hydrotrope-hydrotrope interactions. Furthermore, the model revealed smaller solute-hydrotrope aggregation values for 1,n-alkanediols, which were rationalized in terms of hydrotrope self-aggregation.

Finally, two chemical environment probes were used to confirm the different degrees of self-aggregation for 1,2-alkanediols and 1,n-alkanediols. These results showed that the extent of solute-hydrotrope aggregation is larger in 1,2-alkanediols than in 1,n-alkanediols, which is most noteworthy for high hydrotrope concentration.

## Acknowledgements

This work was developed within the scope of the project CICECO-Aveiro Institute of Materials, UIDB/50011/2020 & UIDP/50011/2020, and CIMO-Mountain Research Center, UIDB/00690/2020, financed by national funds through the FCT/ MEC, and when appropriate, cofinanced by FEDER under the PT2020 Partnership Agreement. B. P. S. acknowledges FCT for her PhD grant SFRH/BD/138439/2018.

## References

- 1 P. Anastas and N. Eghbali, Green Chemistry: Principles and Practice, *Chem. Soc. Rev.*, 2010, **39**, 301–312.
- 2 W. Kunz, K. Holmberg and T. Zemb, Hydrotropes, *Curr. Opin. Colloid Interface Sci.*, 2016, **22**, 99–107.
- 3 R. Paul, K. G. Chattaraj and S. Paul, Role of Hydrotropes in Sparingly Soluble Drug Solubilization: Insight from a Molecular Dynamics Simulation and Experimental Perspectives, *Langmuir*, 2021, **37**, 4745–4762.
- 4 S. Shimizu, Formulating rationally via statistical thermodynamics, *Curr. Opin. Colloid Interface Sci.*, 2020, **48**, 53–64.
- 5 C. Neuberg, Hydrotropische Erscheinungen, *Biochem. Z.*
- 6 T. K. Hodgdon and E. W. Kaler, Hydrotropic solutions, *Curr. Opin. Colloid Interface Sci.*, 2007, **12**, 121–128.
- 7 B. P. Soares, D. O. Abranches, T. E. Sintra, A. Leal-Duaso, J. I. García, E. Pires, S. Shimizu, S. P. Pinho and J. A. P. Coutinho, Glycerol Ethers as Hydrotropes and Their Use to Enhance the Solubility of Phenolic Acids in Water, *ACS Sustain. Chem. Eng.*, 2020, **8**, 5742–5749.
- 8 L. Moity, Y. Shi, V. Molinier, W. Dayoub, M. Lemaire and J.-M. Aubry, Hydrotropic Properties of Alkyl and Aryl Glycerol Monoethers, *J. Phys. Chem. B*, 2013, **117**, 9262–9272.
- 9 R. Lebeuf, E. Illous, C. Dusseune, V. Molinier, E. Da Silva, M. Lemaire and J.-M. Aubry, Solvo-Surfactant Properties of Dialkyl Glycerol Ethers: Application as Eco-Friendly Extractants of Plant Material through a Novel Hydrotropic Cloud Point Extraction (HCPE) Process, *ACS Sustain. Chem. Eng.*, 2016, **4**, 4815–4823.
- 10 A. F. M. Cláudio, M. C. Neves, K. Shimizu, J. N. Canongia Lopes, M. G. Freire and J. A. P. Coutinho, The magic of aqueous solutions of ionic liquids: ionic liquids as a powerful class of catanionic hydrotropes, *Green Chem.*, 2015, **17**, 3948–3963.
- 11 D. O. Abranches, J. Benfica, B. P. Soares, A. M. Ferreira, T. E. Sintra, S. Shimizu and J. A. P. Coutinho, The impact of the counterion in the performance of ionic hydrotropes, *Chem. Commun.*, 2021, **57**, 2951–2954.
- 12 T. E. Sintra, D. O. Abranches, J. Benfica, B. P. Soares, S. P. M. Ventura and J. A. P. Coutinho, Cholinium-based ionic liquids as bioinspired hydrotropes to tackle solubility challenges in drug formulation, *Eur. J. Pharm. Biopharm.*, 2021, **164**, 86–92.

- 13 R. E. Coffman and D. O. Kildsig, Effect of Nicotinamide and Urea on the Solubility of Riboflavin in Various Solvents, *J. Pharm. Sci.*, 1996, **85**, 951–954.
- 14 S. Shimizu and N. Matubayasi, The origin of cooperative solubilisation by hydrotropes, *Phys. Chem. Chem. Phys.*, 2016, **18**, 25621–25628.
- 15 D. O. Abranches, J. Benfica, B. P. Soares, A. Leal-Duaso, T. E. Sintra, E. Pires, S. P. Pinho, S. Shimizu and J. A. P. Coutinho, Unveiling the mechanism of hydrotropy: evidence for water-mediated aggregation of hydrotropes around the solute, *Chem. Commun.*, 2020, **56**, 7143–7146.
- 16 A. Behr, J. Eilting, K. Irawadi, J. Leschinski and F. Lindner, Improved utilisation of renewable resources: New important derivatives of glycerol, *Green Chem.*, 2008, **10**, 13–30.
- 17 B. Ozturk and M. Gonzalez-Miquel, Alkanediol-based deep eutectic solvents for isolation of terpenoids from citrus essential oil: Experimental evaluation and COSMO-RS studies, *Sep. Purif. Technol.*, 2019, **227**, 115707.
- 18 C. Srinivasulu, M. Ramgopal, G. Ramanjaneyulu, C. M. Anuradha and C. Suresh Kumar, Syringic acid (SA) – A Review of Its Occurrence, Biosynthesis, Pharmacological and Industrial Importance, *Biomed. Pharmacother.*, 2018, **108**, 547–557.
- 19 M. J. Kamlet, J. L. Abboud and R. W. Taft, The solvatochromic comparison method. 6. The  $\pi^*$  scale of solvent polarities, *J. Am. Chem. Soc.*, 1977, **99**, 6027–6038.
- 20 D. C. Dong and M. A. Winnik, THE Py SCALE OF SOLVENT POLARITIES. SOLVENT EFFECTS ON THE VIBRONIC FINE STRUCTURE OF PYRENE FLUORESCENCE and EMPIRICAL CORRELATIONS WITH ET and Y VALUES, *Photochem. Photobiol.*, 1982, **35**, 17–21.
- 21 G. T. Hefter and R. P. T. Tomkins, Eds., *The Experimental Determination of Solubilities*, John Wiley & Sons, Ltd, Chichester, UK, 2003.
- 22 D. O. Abranches, J. Benfica, S. Shimizu and J. A. P. Coutinho, The Perspective of Cooperative Hydrotropy on the Solubility in Aqueous Solutions of Cyrene, *Ind. Eng. Chem. Res.*, 2020, **59**, 18649–18658.
- 23 W. E. May, S. P. Wasik, M. M. Miller, Y. B. Tewari, J. M. Brown-Thomas and R. N. Goldberg, Solution thermodynamics of some slightly soluble hydrocarbons in water, *J. Chem. Eng. Data*, 1983, **28**, 197–200.
- 24 R. Zana and M. J. Eljebari, Fluorescence probing investigation of the self-association of alcohols in aqueous solution, *J. Phys. Chem.*, 1993, **97**, 11134–11136.

- 25 M. Vasilescu, D. F. Anghel, M. Almgren, P. Hansson and S. Saito, Fluorescence Probe Study of the Interactions between Nonionic Poly(oxyethylenic) Surfactants and Poly(acrylic acid) in Aqueous Solutions, *Langmuir*, 1997, **13**, 6951–6955.
- 26 Y. Kusumoto, Y. Takeshita, J. Kurawaki and I. Satake, Preferential Solvation Studied by the Fluorescence Spectrum of Pyrene in Water-Alcohol Binary Mixtures, *Chem. Lett.*, 1997, **26**, 349–350.
- 27 J. Setschenow, Über die Konstitution der Salzlösungen auf Grund ihres Verhaltens zu Kohlensäure, *Zeitschrift für Phys. Chemie*, 1889, **4U**, 117–125.
- 28 N. Ni and S. H. Yalkowsky, Prediction of Setschenow constants, *Int. J. Pharm.*, 2003, **254**, 167–172.
- 29 S. Abbott, J. J. Booth and S. Shimizu, Practical molecular thermodynamics for greener solution chemistry, *Green Chem.*, 2017, **19**, 68–75.
- 30 D. O. Abranches, J. Benfica, S. Shimizu and J. A. P. Coutinho, Solubility Enhancement of Hydrophobic Substances in Water/Cyrene Mixtures: A Computational Study, *Ind. Eng. Chem. Res.*, 2020, **59**, 18247–18253.
- 31 I. K. Yoo, J. H. Kim and Y. K. Kang, Conformational preferences and antimicrobial activities of alkanediols, *Comput. Theor. Chem.*, 2015, **1064**, 15–24.
- 32 S. P. Verevkin, Determination of vapor pressures and enthalpies of vaporization of 1,2-alkanediols, *Fluid Phase Equilib.*, 2004, **224**, 23–29.
- 33 P. Umnahanant, S. Kweskin, G. Nichols, M. J. Dunn, H. Smart-Ebinne and J. S. Chickos, Vaporization Enthalpies of the  $\alpha,\omega$ -Alkanediols by Correlation Gas Chromatography, *J. Chem. Eng. Data*, 2006, **51**, 2246–2254.
- 34 W. E. Acree, S. A. Tucker and D. C. Wilkins, Spectrochemical investigations of preferential solvation: fluorescence emission behavior of select polycyclic aromatic hydrocarbon solute probes dissolved in mixed solvents, *J. Phys. Chem.*, 1993, **97**, 11199–11203.
- 35 W. E. Acree, D. C. Wilkins, S. A. Tucker, J. M. Griffin and J. R. Powell, Spectrochemical Investigations of Preferential Solvation. 2. Compatibility of Thermodynamic Models versus Spectrofluorometric Probe Methods for Tautomeric Solutes Dissolved in Binary Mixtures, *J. Phys. Chem.*, 1994, **98**, 2537–2544.